

# Mesoscopic Fluctuations of Electronic Structure Properties of Boron Phosphide Nanocrystals

Mudar A. Abdulsattar\*

Ministry of Science and Technology, Directorate of Materials Science, Baghdad, Iraq

The ab initio restricted Hartree-Fock method is used to simulate the electronic structure of relatively large boron phosphide nanocrystals (216-1000 atoms). The calculations are divided into two parts, surface and core. Nanocrystals are found to have smaller lattice constants and higher ionicity as they increase in size. The core calculations show increasing energy gap, cohesive energy, and valence bandwidth as well as highly degenerated states with increasing nanocrystal size. The energy gap, cohesive energy, and valence bandwidth have damping fluctuations as these quantities converge to constant bulk values as the nanocrystal reaches a high number of atoms. These fluctuations are similar to mesoscopic fluctuations that converge to bulk values and are related to the geometry and various surfaces of the core. Unlike the core part, the hydrogenated B-terminated (001)-(1×1) surface of these crystals has a smaller energy gap, and wider valence and conduction bands. Reduced symmetry caused less degenerate states to occur at the surface. Having slightly different lattice constants, both core and shell parts experience stresses to match each other dimensions. On the other hand, unlike the energy gap, the ionization potentials and affinity do not converge to a unique value as the core of nanocrystals increases in size because of the different surfaces that bound these nanocrystals.

**Keywords:** nanocrystals, abinitio calculations, semiconductors

## 1. INTRODUCTION

Cubic boron phosphide (c-BP) semiconductors have been repeatedly reported to show excellent device properties for a variety of applications, such as light emitting diodes (LEDs) or laser diodes (LDs),<sup>[1]</sup> and they are considered an important wide-gap semiconductor in the electronics industry. Nanocrystals of c-BP have been recently synthesized in various sizes by various methods.<sup>[2,3]</sup> This compound is one of the nearest zinc-blend structures to the covalent diamond-structured elements (diamond, silicon, germanium, and  $\alpha$ -tin) because of its small ionicity. Unlike diamond-structured elements and many zincblend compounds, this compound had received very limited attention in theoretical and practical investigations as a low-dimensional structure. In this work we shall investigate the electronic structure of relatively large c-BP nanocrystals using the large unit cell method (LUC) for the core and surface parts (Figs. 1 and 2). The LUC method is traditionally used to simulate bulk and surface parts of ordinary size crystals.<sup>[4,5]</sup> The LUC differs from other supercell methods by the use of  $\mathbf{k} = 0$  approximation ( $\mathbf{k}$  is the lattice wave vector) with no summation over  $\mathbf{k}$  space. Instead of adding additional  $\mathbf{k}$  points to the reciprocal space, the number of atoms in the central cell ( $\mathbf{k} = 0$ ) is

increased, and a larger central unit cell is formed.

The LUC method was first suggested and applied to covalent semiconductors in the 1970s.<sup>[4,5]</sup> This method was found suitable for nanocrystal calculations because the  $\mathbf{k} = 0$  approximation retains only one central cluster of atoms surrounded by other atoms to passivate the outer dangling bonds.<sup>[6,7]</sup> The method is used to simulate parts of specific symmetry in the nanocrystal in the same way it is used for bulk materials.

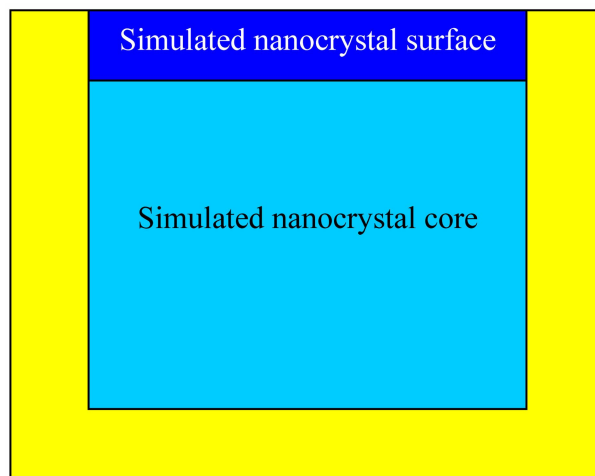


**Fig. 1.** (Color online) A cross section of a hypothetical cubic Nanocrystal geometry as applied to the present work calculations.

\*Corresponding author: mudarahmed3@yahoo.com

## 2. THEORY

The electronic structure of the c-BP nanocrystals of increasing size is investigated using the ab initio restricted Hartree-Fock method available in the Gaussian 03 program.<sup>[8]</sup> The investigation includes both Bravais and primitive cell multiples.<sup>[9]</sup> The calculations were carried out for the core and shell (surface) geometries as shown in Figs. 1 and 2. The core part of the nanocrystal should have a nearly perfect zincblend structure (Fig. 2(a)). This part is one lattice constant away from the surface to prevent surface effects.<sup>[9]</sup> The surface part is investigated using slab geometry as shown in Fig. 2(b).

The minimum number of atoms in a cubic nanocrystal (Fig. 1) is 216 so that it can have a core (8 atoms) that is one lattice apart from the surface. The investigated numbers of core atoms are 8, 64, and 216 for the Bravais cell and 16, 54, and 128 for the primitive cell multiples.<sup>[9]</sup> The largest num-

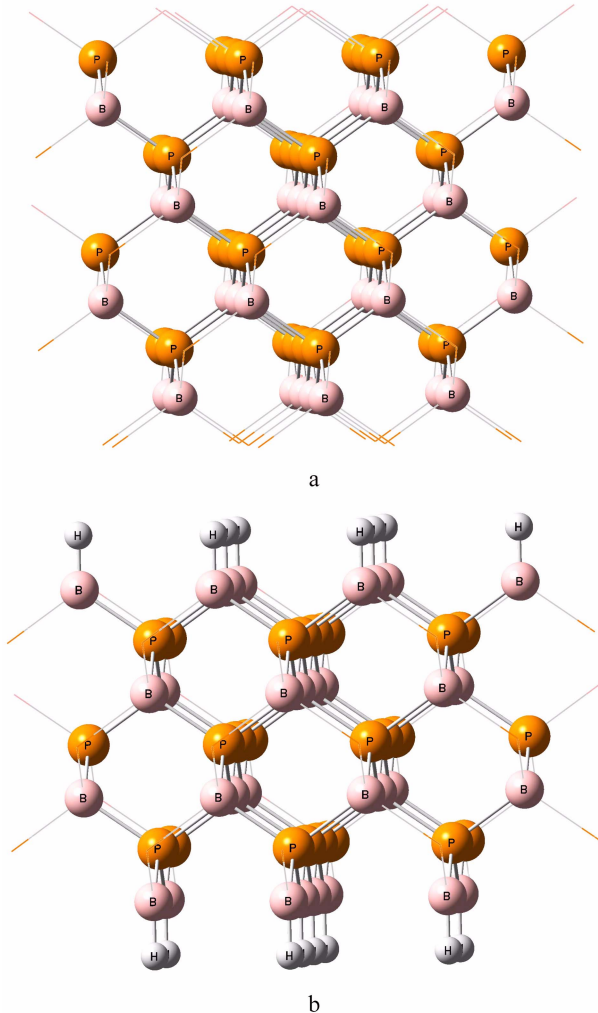


**Fig. 2.** (Color online) a- The 64 atom c-BP core LUC. b- Hydrogenated B-terminated (001)-(1×1) surface slab of  $B_{32}H_{16}P_{24}$  stoichiometry.

ber of core atoms investigated in the present work (216 atoms) corresponds to 1000 atoms for the total number of atoms in the nanocrystal. This number is rarely investigated using ab initio calculations.

Two surface stoichiometries are investigated, namely,  $B_8H_4P_6$  and  $B_{32}H_{16}P_{24}$ . These hydrogenated B-terminated (001)-(1×1) surfaces serve as an example for the effect of the surface on the overall electronic structure of the nanocrystal.

## 3. CALCULATIONS AND RESULTS

The lattice constant of the cores of nanocrystals of various sizes are energetically optimized as shown in Fig. 3. The optimization shows that the smallest investigated nanocrystal core (8 atoms) has a lattice constant that is nearly 2.7% larger than the converging lattice constant value for larger nanocrystals. The converged lattice length for a high number of core atoms (4.51 Å) is in good agreement with the experimentally reported value (4.53 Å) for large nanocrystals<sup>[2,3]</sup> and bulk.<sup>[10]</sup> Figures 4, 5, and 6 show energy gap, cohesive energy, and valence bandwidth variation as the nanocrystals core increases in size. All energies converge quickly for the crystals with more than 50 core atoms with a very narrow energy gap variation range (4.64 eV to 4.68 eV). The energy gap is higher than the experimentally reported energy gap (2.0 eV) for bulk c-BP<sup>[10]</sup> but within the trends of Hartree-Fock theory of giving high energy gaps.<sup>[6,7]</sup> The converged cohesive energy and valence bandwidth (14.5 eV and 16.8 eV respectively) are comparable to the bulk experimental values of 10.24 eV and 16.5 eV respectively.<sup>[10,11]</sup> Cohesive energy and valence bandwidth have similar fluctuations to that of the energy gap. These fluctuations are similar to mesoscopic fluctuations that converge to bulk values and are related to the geometry of the core LUCs. Geometric differences originate from the different terminating surfaces of these Bravais or primitive cells.

Figure 7 shows the ionicity of the core part of nanocrystals

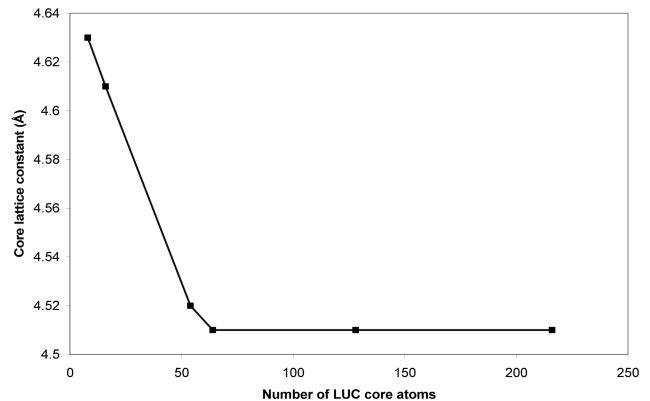


**Fig. 3.** Energetically optimized c-BP core lattice constant as a function of the number of atoms in the core.

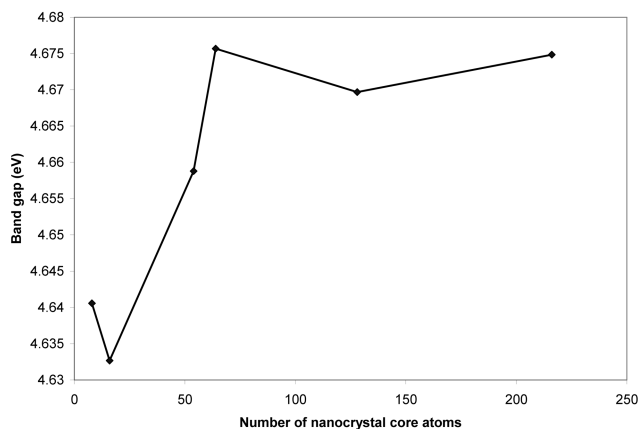


**Fig. 4.** Energy gap of the core part of c-BP nanocrystals as a function of the number of core atoms.

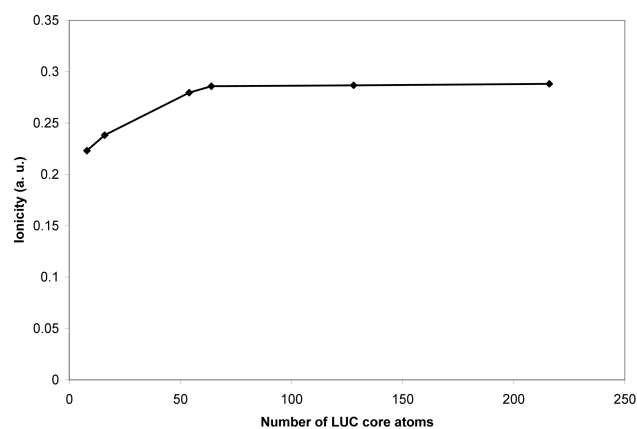


**Fig. 7.** Ionicity of the core part of c-BP nanocrystals as a function of core atoms.

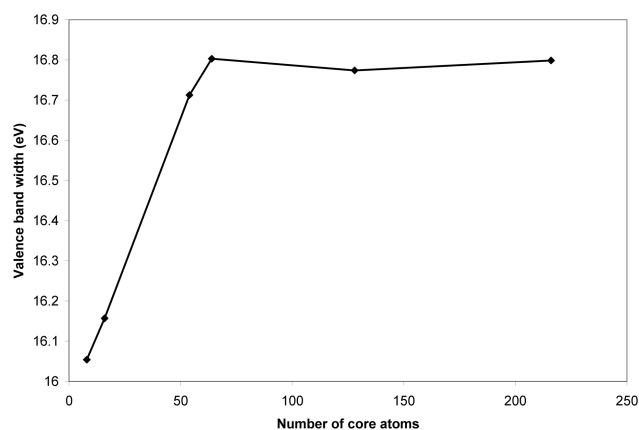


**Fig. 5.** Valence band width of the core part of c-BP nanocrystals as a function of core atoms.

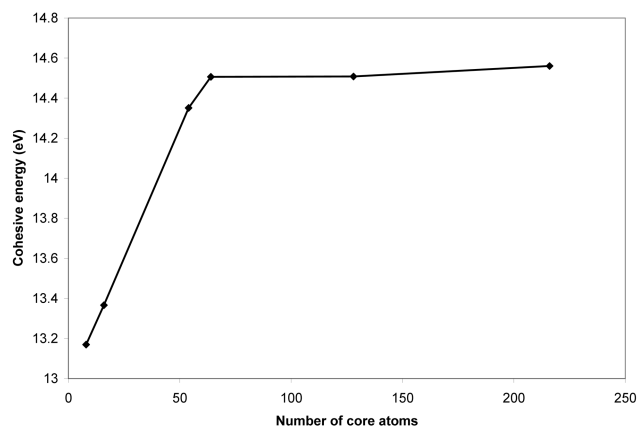


**Fig. 6.** Cohesive energy of the core part of c-BP nanocrystals as a function of the number of core atoms.

as they increase in size. This figure shows that smaller nanocrystals are less ionic than larger nanocrystals. This can be attributed to the larger lattice constant in smaller nanocrystals and the consequent lower electronic interaction. The

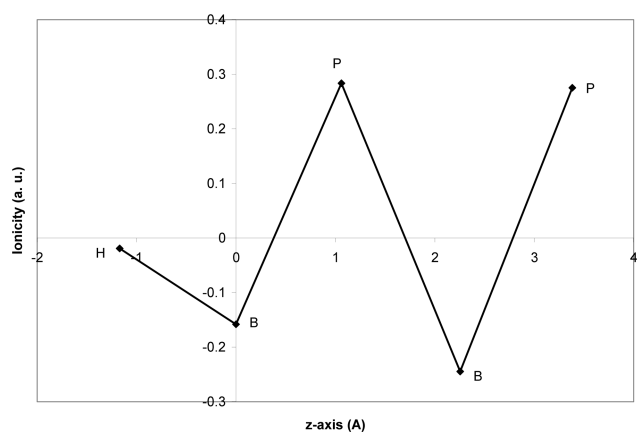


**Fig. 8.** Atomic ionicity as a function of layer depth perpendicular to the hydrogenated B-terminated (001)-(1×1) c-BP for the  $B_{32}H_{16}P_{24}$  stoichiometry slab surface.

converged value of 0.29 for large nanocrystals is in good agreement with the bulk experimental value of 0.25.<sup>[12]</sup> Figure 8 also shows the atomic ionicity of atomic layers perpendicular to the (001) surface. The layer at 0 coordinates is the first boron layer which has negative atomic ionicity. The hydrogen atom layer at the left side of 0 coordinate layer also has negative ionicity. The first phosphorus layer at the right of the 0 coordinate layer has positive ionicity. The layers beyond this layer have alternately negative and positive atomic charges.

Due to high symmetry, the number of degenerate states is high in the core part (Fig. 9). The highest number of degenerate states in the valence band is between 6 for the 8 atom core and 36 for the 216 atom core. These numbers are in excellent agreement with the same results using semiempirical methods for diamond-structure elements.<sup>[7]</sup>

To investigate nanocrystals surface electronic structure, it is natural to assume that larger nanocrystals to have larger surfaces. Two hydrogenated B-terminated (001)-(1×1) c-BP

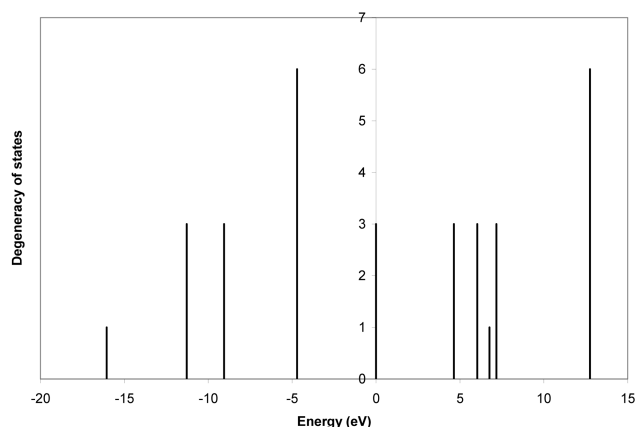


**Fig. 9.** Degeneracy of states of 8 atom core part of c-BP nanocrystal as a function of level energy. The HOMO level is taken as the reference level.

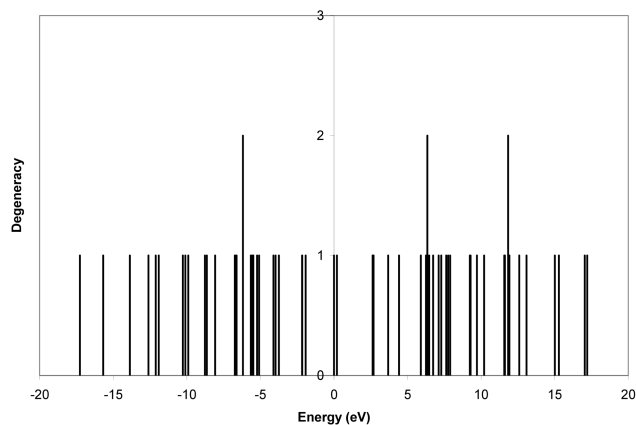


**Fig. 10.** Degeneracy of states of surface part of  $B_8H_4P_6$  stoichiometry slab as a function of level energy. The HOMO level is taken as the reference level.

surface stoichiometry slabs are investigated, namely,  $B_8H_4P_6$  and  $B_{32}H_{16}P_{24}$  (Fig. 2b) with two surface areas of  $a^2$  and  $4a^2$  respectively, where ( $a$ ) is the lattice constant. The B-H bond length is optimized to 1.17, which is in good agreement with experimental value for  $BH_3$  of 1.19 Å.<sup>[13]</sup> The bond lengths and angles at the surface are not unique as in the core part. Due to symmetry considerations, only inter-layer distances in the vertical direction in Fig. 2(b) are affected. The distance between the second and third layers in Fig. 2(b) (assuming the H atoms to be in the first layer) is 6 % shorter than the ordinary 1.1275 Å distance between these layers (with the exception of the hydrogen layer). The geometry and second to third layer distance contraction is similar to the oxygenated diamond surface in the ketone (C = O) case.<sup>[14]</sup> The average lattice constants of the two investigated stoichiometries are 4.51 Å and 4.48 Å, which are less than the corresponding core parts (8 atoms and 64 atoms), but they follow the same decreasing order. This shows that both core and shell parts experience stress to match each other's dimensions. Unlike the core part, the highly degenerate states of the core are split and the energy gap is reduced (Fig. 10). The highest numbers of degenerated states in the two investigated stoichiometries are 2 and 4, respectively. The energy gaps of the two stoichiometries are 0.2 eV and 1.0 eV, respectively. This increasing energy gap with increasing surface area is in agreement with results for similar size diamond nanocrystals which show the same trend beyond the quantum confinement region.<sup>[15]</sup>

Due to level splitting, the valence and conduction bands are also widened. The low surface energy-gap values show that the energy gap is ruled by the surface part of the nanocrystals, and this is in agreement with diamond results.<sup>[15]</sup>

Other quantities that can be obtained from our calculations are the ionization potential and affinity. Affinity is the energy difference when an electron is brought from infinity to the

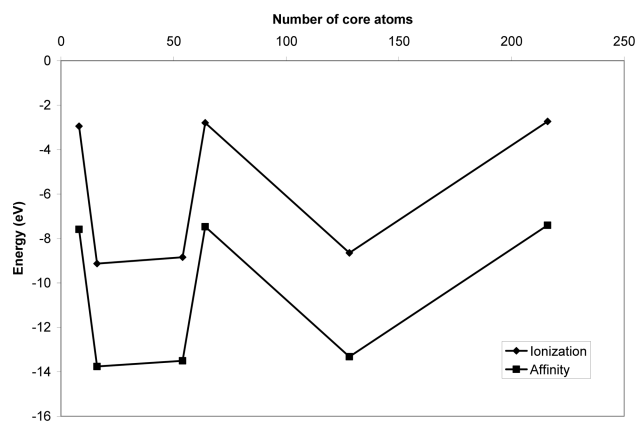


**Fig. 11.** Ionization and affinity as a function of the number of core atoms.

material, while ionization potential is the energy difference when an electron is removed from the material to an infinite- or zero-potential state. Figure 11 shows these quantities for the core part of the nanocrystal. The difference between ionization potential and affinity is almost constant and is equal to the value of the energy gap as a first approximation.<sup>[14]</sup> In spite of the oscillation of these quantities, these oscillations do not vanish as the core of the nanocrystal expands (compare to energy gap Fig. 4). Note that the first, fourth, and sixth data points of the Fig. 11 are Bravais LUCs (8 atoms, 64 atoms, and 216 atoms), and they have nearly distinct constant values that differ from the second, third, and fifth data points, which are primitive LUCs (16 atoms, 54 atoms, and 128 atoms, respectively). Since each of the Bravais and primitive cells is bounded by different surfaces in the nanoscale and bulk scale, the difference in electron affinity and ionization potential remains.

The surface ionization and affinity values are 2.75 eV and 2.54 eV for the  $B_8H_4P_6$  stoichiometry and 2.33 eV and 1.29

eV for the  $B_{32}H_{16}P_{24}$  stoichiometry, respectively. Unlike the core, the values of surface ionization and affinity are all positive for this surface and are nearer to the 0 potential in vacuum in their values as well as their spatial position.

#### 4. CONCLUSIONS

In conclusion, smaller nanocrystals are found to have larger lattice constants and a less ionic character. The core part shows damping oscillations for the energy gap and other electronic structure energy properties, such as cohesive energy and valence band-width. These fluctuations are similar to mesoscopic fluctuations that converge to bulk values and are related to the geometry of the core LUCs (Bravais or primitive cells). It also shows an increasing general trend for the cohesive energy, valence bandwidth, and highly degenerated states to converge rapidly to bulk properties with increasing nanocrystal size. Unlike the core part, the hydrogenated B-terminated (001)-(1×1) surface of these crystals has a lower energy gap, wider valence and conduction bands, and less degenerate states. Having slightly different lattice constants, both core and shell parts experience stresses to match each other's dimensions. On the other hand, other physical quantities at the core such as ionization potential and affinity do not show the same convergence as the energy gap, cohesive energy, and valence bandwidth. However, ionization and affinity values oscillate according to the geometry, surface, and shape of the nanocrystal core.

#### REFERENCE

1. T. Udagawa, *US Patent 7508010 B2* (2009).
2. L. Y. Chen, Y. L. Gu, L. Shi, J. H. Ma, Z. H. Yang, and Y. T. Qian, *Chem. Lett.* **32**, 1188 (2003).
3. X. Feng, L. Y. Shi, J. Z. Hang, J. P. Zhang, J. H. Fang, and Q. D. X. Zhong, *Mater. Lett.* **59**, 865 (2005).
4. A. Dobrotvorski and R. Evarestov, *Phys. Status Solidi B* **66**, 83 (1974).
5. A. Harker and F. Larkins, *J. Phys. C* **12**, 2487 (1979).
6. M. A. Abdulsattar and K. H. Al-Bayati, *Phys. Rev. B* **75**, 245201 (2007).
7. M. A. Abdulsattar, *Physica E* **41**, 1679 (2009).
8. M. J. Frisch, G. W. Trucks, H. B. Schlegel, G. E. Scuseria, M. A. Robb, J. R. Cheeseman, J. A. Montgomery, Jr., T. Vreven, K. N. Kudin, J. C. Burant, J. M. Millam, S. S. Iyengar, J. Tomasi, V. Barone, B. Mennucci, M. Cossi, G. Scalmani, N. Rega, G. A. Petersson, H. Nakatsuji, M. Hada, M. Ehara, K. Toyota, R. Fukuda, J. Hasegawa, M. Ishida, T. Nakajima, Y. Honda, O. Kitao, H. Nakai, M. Klene, X. Li, J. E. Knox, H. P. Hratchian, J. B. Cross, C. Adamo, J. Jaramillo, R. Gomperts, R. E. Stratmann, O. Yazyev, A. J. Austin, R. Cammi, C. Pomelli, J. W. Ochterski, P. Y. Ayala, K. Morokuma, G. A. Voth, P. Salvador, J. J. Dannenberg, V. G. Zakrzewski, S. Dapprich, A. D. Daniels, M. C. Strain, O. Farkas, D. K. Malick, A. D. Rabuck, K. Raghavachari, J. B. Foresman, J. V. Ortiz, Q. Cui, A. G. Baboul, S. Clifford, J. Cioslowski, B. B. Stefanov, G. Liu, A. Liashenko, P. Piskorz, I. Komaromi, R. L. Martin, D. J. Fox, T. Keith, M. A. Al-Laham, C. Y. Peng, A. Nanayakkara, M. Challacombe, P. M. W. Gill, B. Johnson, W. Chen, M. W. Wong, C. Gonzalez, and J. A. Pople, *Gaussian 03, Revision B.01*, Gaussian, Inc., Pittsburgh PA, (2003).
9. C. Kittel, *Introduction to Solid State Physics, 5th ed.*, Wiley, New York (1976).
10. R. M. Wentzcovitch, K. J. Chang, and M. L. Cohen, *Phys. Rev. B* **34**, 1071 (1986).
11. S. Bađci, S. Duman, H. M. Tütüncü, and G. P. Srivastava, *Phys. Rev. B* **79**, 125326 (2009).
12. P. J. Gielisse, S. S. Mitra, J. N. Plendl, R. D. Griffis, L. C. Mansur, R. Marshall, and E. A. Pascoe, *Phys. Rev.* **155**, 1039 (1967).
13. J. Karlsson and K. Larsson, *J. Phys. Chem. C* **114**, 3516 (2010).
14. S. J. Sque, R. Jones, and P. R. Briddon, *Phys. Rev. B* **73**, 085313 (2006).
15. J. Y. Raty, G. Galli, C. Bostedt, T. W. vanBuuren, and L. J. Terminello, *Phys. Rev. Lett.* **90**, 037401 (2003).